Dynamics of current-sharing within a REBCO tape-stack cable

J.S. Rogers, G.D. May, C. D. Coats, and P.M. McIntyre, *Fellow, IEEE*

***Abstract*— Current redistribution in a non-insulating REBCO tape-stack cable may enable the use of such a cable in a high field dipole without provision for transposition of the constituent tapes.As current is increased in the REBCO cable a dynamic resistance arises in the superconductinglayer near operation at critical current. The critical current of each tape in the stack varies according to the local magnetic field on the cable. The superconducting-normal transition in REBCO occurs over a working range of current and, within that range, the longitudinal Ohmic electric field produces a transverse electric field between adjacent tapes with different critical currents. Circuit models indicate that, as a given tape approaches critical operation, current will naturally redistribute to neighboring tapes with higher current carrying capacity due to the dynamic rise in resistivity thus preventing premature quench. A multi-scale model is being developed to study the dynamics of current-sharing, the limits of stability, and the impact of fluctuations in critical-current density along each tape.**

1

***Index Terms*— Accelerator magnets, Superconducting magnets, HTS Coils, No-insulation coils, Superconducting coils**

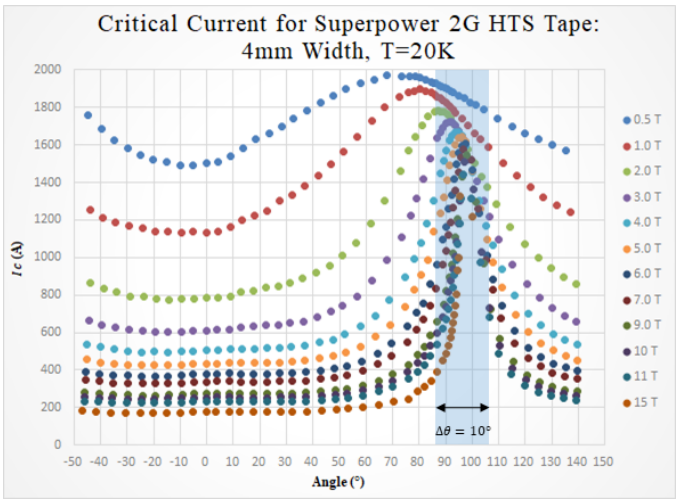

Fig. 1. Dependence of critical current on field strength and orientation in high-performance Superpower 4 mm-wide REBCO tape at 20 K. [1]

I. Introduction

RARE-EARTH Barium Copper Oxide (REBCO) is a class of high-temperature superconductors (HTS) that can maintain appreciable current density in both high-field and high-temperature environments. Recent advancements in fabrication technology for HTS wires have resulted in dramatic improvement in critical current and wire length [1,2].

The properties of REBCO make it beneficial for use in high-field magnets [3,4] notably in non-insulating (NI) double-pancake windings ('pucks') [5] of a solenoid. It has been shown that, under certain conditions, currents can redistribute among layers in a NI winding during ramping and discharge [6].

This capacity for current sharing has inspired development of an NI REBCO cable and a magnetic design of a conformal insert winding for a high-field hybrid dipole. In this work the dynamics of current-sharing in thiscable has been modeled and investigated during ramping and steady-state operation.

II. REBCO Tapes

REBCO conductor is typically fabricated in a tape geometry in which a thin superconducting film is deposited onto a Hastelloy substrate and then Ag and Cu matrix layers are bonded to form a hermetic sheath [1]. The tape cannot be bent in its *a-b* plane *i.e.* the 'hard-direction' without incurring damage.

For applications that require a single tape conductor, the tape is usually spiral-wrapped into a winding. For some applications an electrically insulating layer can be coated on the tape surfaces, or the tape can be co-wound or wrapped with an insulating material. Alternatively, tapes can be wound without insulation such that they are in direct electrical contact between turns; this is the case for NI solenoid windings [5].

For applications that require a large winding current, multiple tapes are packaged as a cable, using any of a variety of strategies: twisted-stack [7,8], Roebel [9,10], CORC© [11,12], and VIPER [13]. In all of these cables, the tapes within the cable are transposed – each tape traverses within the cable so that it spends an equal length on the inside and outside region of the cable along the winding length.

This work was supported by U.S. Department of Energy SBIR grant to ATC: DDE-SC0021688 – "Nb3Sn SuperCIC outsert and REBCO conformal insert for an 18 T collider dipole", and U.S. Department of Energy research grant to Texas A&M University: DE-SC0023028 – "Conformal REBCO windings For high-field dipoles"

J.S. Rogers, G.D. May, C. Coats, and P. McIntyre are with Texas A&M University Department of Physics and also are with Accelerator Technology Corporation, College Station, TX 77845, USA (e-mail: johnrogers@tamu.edu)

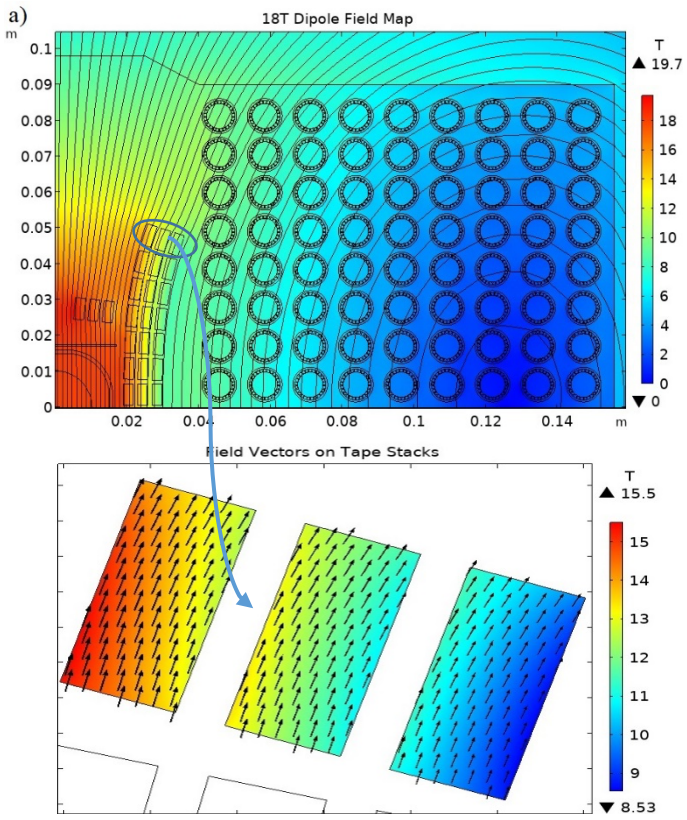

Fig. 2. a) Quadrant cross-section of the 18 T hybrid dipole with conformal REBCO insert and Nb3Sn SuperCIC outsert originally presented in Ref. 14.

REBCO is a highly anisotropic superconductor: its critical current I_c is strongly dependent on the strength and the angle of the magnetic field on the tape (Fig. 1). Alas, REBCO is also notoriously expensive.

The state of the art for modern high-field cable-based REBCO technology is under the conviction that one must transpose the cable and thus must settle for an operating current that is not much better than the minimum shown in Fig. 1. The above considerations led us to design a quite different strategy [14] in which

- the tapes in the cable are not transposed;
- all tapes are oriented such that the tape faces are nearly parallel with the local magnetic field in the winding;
- current sharing is driven by the dynamic rise in resistivity near the normal-superconducting transition to naturally redistribute currents within the cable as current is increased.

This paper primarily addresses the third stratagem.

A. Tape-Wound NI Solenoids

HTS NI solenoids are typically configured as a coaxial stack of double-pancake windings (pucks) of REBCO tape with face-to-face radial contact between the adjacent turns within a puck. Since there is no insulation from turn-to-turn the tape faces are in electrical contact and can readily share current between tape layers; this property provides for enhanced stability against quench but also has produced time-changing patterns during quench in NI solenoids [15,16,17]. For example, current may start flowing radially through the spiral winding instead of azimuthally as desired.

Current sharing through face contact between neighboring REBCO tapes is driven by the dynamic rise in resistivity near critical operation, the Hall effect, and (during ramping) by inductive coupling between tape layers. These mechanisms rely upon flux penetration within the superconducting layer of the REBCO tape. Flux penetration has been studied both experimentally and theoretically [18], but is still not well understood. Future experiments presented in Sec. V will further investigate the role of Hall-like effects and inductive coupling in NI REBCO coils.

TABLE I
SPECIFICATIONS FOR 18 T HYBRID DIPOLE

	REBCO Insert	Nb_3Sn Outsert
Cable Current (I_{op})	18 kA	18 kA
Cable Critical Current (I_c)	21038 A	20969 A
Current Operating Margin	0.86	0.86
Peak Field on Cable	18.3 T	11.1 T
Operating Temp.	20 K	5 K
Wire Manufacturer	SuperPower Inc.	Bruker OST LLC
Wire Specifications	2G HTS Tape 50 µm Cu clad	RRP 108/127 Cu/SC=1.17
Wire Dimensions	0.1 mm x 6 mm	0.85 mm OD
#Wires in Cable	28	26
# Cable Turns/bore	48	144

B. Dipoles with NI REBCO Transposed Cables

Recently, there has been significant interest in using REBCO based windings for the next generation of very-high-field dipoles (16 T+). Designs have been proposed for exclusively REBCO based windings [19] as well as hybrid dipoles using HTS inserts with LTS outserts [20].

In [21] a dipole insert winding (the 'Feather dipole') was built and tested in which a REBCO Roebel cable was configured so that the *a-b* plane of the tapes are approximately aligned with the local magnetic field. Although the cables are oriented with the tapes of each cable approximately parallel to the local field, each tape folds twice in each transposition, and during fold the tape face is in the worst orientation.

Another example is the 2.9 T dipole built and tested using CORC© cable in [22]. Current transfer occurs readily among adjacent tapes within each cable, but all tapes spend an equal length in all orientations with respect to the local field so operating current is limited to approximately the average of the values in the best and worst orientations.

III. MAGNETIC DESIGN FOR CONFORMAL HYBRID DIPOLE

Our recent paper [14] presented a design for an 18 T hybrid dipole in which conformal winding and current sharing are optimized. Fig. 2 Fig. 2. a) Quadrant cross-section of the 18 T

hybrid dipole with conformal REBCO insert and Nb3Sn Super-CIC outsert originally presented in Ref. 14.shows a quadrant cross-section of the dipole.

It contains an insert winding made from rectangular REBCO tape-stack cable and an outsert winding made from Nb_3Sn Cable-in-Conduit 'SuperCIC' [23]. Table I summarizes the main parameters of both windings.

The insert winding is contoured so that each tape-stack cable is oriented that the tape faces are closely parallel to the local magnetic field [24]. Fig. 2(b) shows a detailed view of the field orientation in three of the tape-stack cables. The tapes in the inner cable layer operate in high field (where the angular dependence of I_c in Fig. 1 sharply peaks near 90°), and their faces are closely parallel to the magnetic field. Some tapes in the outer cable layer are slightly misaligned to the magnetic field $\vec{B}$, but the magnitude of the field at those tapes is much lower and the angular dependence is broader.

A natural consequence of the conformal insert topology is that it produces a nearly pure dipole field in the bore. Fig. 4 shows the calculated multipoles as a function of current; all values are modest over the entire dynamic range of the dipole. Furthermore, the redistribution of current from outside toward center of each cable does not perturb the multipoles since all such contours are conformal. Persistent-current multipoles, magnetization effects, and AC losses are strongly suppressed [25] because the tapes locally align with the magnetic field.

This hybrid dipole with its conformal REBCO winding is the basis for the current-sharing model presented in Sec. IV.

A. REBCO Tape-Stack Insert Winding

The REBCO tape-stack cable consists of a stack of 28 parallel Cu-clad SuperPower [26] REBCO tapes in face-to-face contact *without transposition*. The tape-stack is preloaded with a face-on compression >1 MPa everywhere in the winding to ensure that neighboring tapes are in electrical contact with low contact resistance R_c between neighboring Cu claddings.

B. Nb_3Sn SuperCIC Outsert Winding

The SuperCIC [23] cable contains 24 RRP Nb_3Sn/Cu wires, spiral-wrapped as a single layer around a thin-wall perforated center tube, then pulled as loose fit through a bronze sheath tube and drawn to compress the wires against the center tube to immobilize them. The outsert winding contributes ~10 T to the central bore field and is being developed in parallel in [27] where magnetic, structural, and fabrication specifications are detailed for the outsert winding.

IV. Dynamics of Current Sharing

A. Current Sharing Within a Stacked Tape Cable

Traditionally the wires in a superconducting cable for high-field magnets are transposed so that each wire is located for equal lengths on the inside and outside of the cable. To visualize the motivation for transposition, consider the Lorentz forces

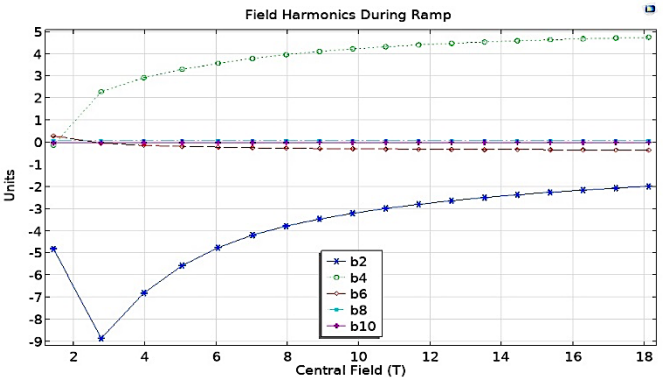

Fig. 3. Field harmonics for a varying range of central bore field. All higher multipoles are <10 units during ramp and <5 units at operating field.

that would act upon the charge carriers if magnetic flux penetrated the tape (a 'perfect conductor' rather than a superconductor). The Lorentz force would tend to drive current from the inner tapes to the outer tapes of each cable. As the field strength increases during ramping, the current in an outer tape would reach its critical current, $I_c(B,T,\theta)$, and cause that tape to quench prematurely.

But the REBCO layer within a tape does not quench abruptly as current increases; it develops a retarding longitudinal electric field E_z that is current dependent: $E_z=E_c(I/I_c)^n$ where E_c = 100 μV/m is the criterion for the critical current, I_c is the critical current for the parameters (B,T,θ) at that location on that tape, and n~30-35 is the index that characterizes the transition.

The dynamics of current distribution incudes a Hall effect in which the superconducting transport is acted upon by the outward Lorentz force, and an inward force produced by the potential difference between neighboring tapes. The current redistributes among the tapes to sustain an equilibrium between these forces, so that the cable current can be increased close to the sum of the critical currents of all tapes without quenching.

B. Estimating Critical Current

To estimate the critical current of each tape in a cable, the critical current density is approximated as a (1-dimensional) sheet critical current density $K_c(\vec{B})$. Next, define the u-axis to run parallel with the REBCO layer in a given tape. The critical current for a given tape is calculated by integrating over the width, W, of that tape:

$$I_c = \int_0^W K_c[\vec{B}(u)]du \qquad (1)$$

The critical current of the cable is given by the summing the individual critical currents of its constituent tapes. It should be noted that this assumes that current can naturally redistribute within the REBCO layer according to a field distribution across the width of a tape. The sheet critical current density, $K_c(\vec{B})$, comes from an interpolated fit of SuperPower [26] experimental critical current data as a function of field magnitude and angle at a fixed temperature (T=20 K) as shown in Fig. 1.

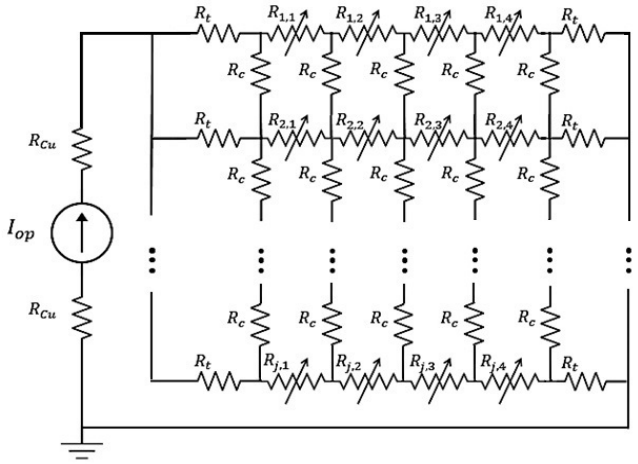

Fig. 4. Circuit model to investigate current sharing in an NI tape-stack cable.

TABLE II
CIRCUIT ELEMENT PARAMETERS

	Symbol	Value
Tape Length	L	10 m
Tape Width	W	6 mm
Lengthwise Divisions	N	4
Quench Criterion	E_c	100 μV/m
n-value	n	35
Tape Contact Resistivity	ρ_c	35 μΩ•cm^2
Solder Join Resistivity	ρ_t	.05 μΩ•cm^2
Terminal Splice Length	L_t	100 mm
Terminal Splice Width	W_t	6 mm
Terminal Resistance	R_t	8.3 nΩ
Contact Resistance	R_c	292 nΩ

C. *Resistive Circuit Model*

. Martinez *et al* [28] developed a circuit model to simulate current sharing between 2 face-to-face tapes around a local defect in I_c. The defect was induced by purposefully damaging one of the tapes and the experiment was performed without external fields.

We have modified this circuit model to simulate a stack of 28 tapes in fac-to-face contact with a gradient in I_c values across the tape-stack due to the magnetic field gradient $\partial B_z / \partial B_x$. The purpose of this model is to investigate redistribution of current during operation of a NI non-transposed tape-stack cable in a conformal winding. The circuit model shown in Fig. 5 simulates the behavior of a straight length of cable corresponding to the midplane inner-most turn of cable in the HTS insert (the segment of cable in highest magnetic field). Although the present model does not represent an entire winding, it faithfully models the experiment proposed in Sec. V.

An ideal power supply acts as the current source through the tape circuit network. Resistors R_{Cu} and R_t represent the resistance of the Cu splice blocks and the terminals respectively. The terminal resistances are calculated using the terminal resistivity ρ_t of a solder lap joint as measured in [29]. The length L and width W must also be specified for the overlapping region of the splice. Note that it is important to design the leads with a sufficiently low value of R_t and to locate the leads in a field-free region, so that current is distributed nearly equally into and out of all 28 tapes of each tape-stack cable.

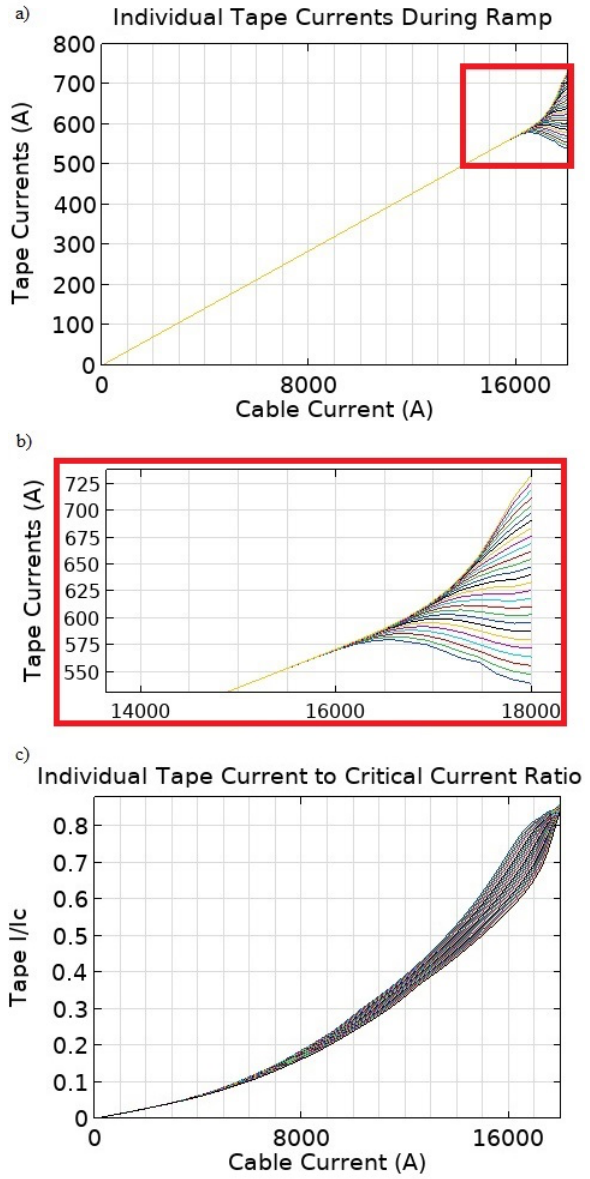

Fig. 5. (a) Individual tape currents during a current ramp. At low current all tapes carry the same current; at high cable current individual currents redistribute and prevent any individual tape from quenching. (b) current redistribution among the tapes with varying I_c values near critical operation. (c) Ratio of I/I_c for all tapes in the cable. At maximum current the operating ratio is nearly the same for all tapes in the cable.

Resistors labeled R_c represent the resistance associated with the REBCO-to-substrate oriented electrical contact between tapes. A laminar spring runs along the length of each of the innermost tape-stack cables to maintain a uniform compression of >1 MPa, thus maintaining electrical contact resistivity ρ_c as demonstrated in [30]. The tapes have width W, and are divided along their length L into N equal segments. Thus,

$$R_t = \frac{\rho_t}{L_t W_t}, \qquad R_c = (N+1)\frac{\rho_c}{LW} \ . \tag{2}$$

The variable resistors, $R_{j,k}$, represent the current dependent rise in resistivity according to the power law as shown below in Eq. (3). $I_{j,k}$ is the current flowing through segment k of tape j

and $I_{c,j}$ is the critical current of tape j as calculated from the magnetic field model:

$$R_{jk} = \frac{V_0}{I_{jk}}\left(\frac{I_{jk}}{I_{c,j}}\right)^n, \qquad V_0 = E_c\left(\frac{L}{N}\right) \tag{3}$$

The values of these parameters are detailed in Table II. At each step in the current ramp the magnetic field model is evaluated, the array $I_{c,j}$ is calculated at that step, and the circuit model is run. Fig. 6(a) shows the current I_{jk} that each tape is carrying as the operating current is ramped up. At cable currents much less than the cable critical current all tapes carry equal amounts of current since all of their resistances are nearly zero. As the cable current approaches its critical value (Fig. 5b) the non-uniform values of R_{jk} drive current redistribution so that tapes with larger $I_{c,j}$ carry more current and vice-versa. Thus current sharing prevents any individual tape from undergoing quench and maximizes the cable current by optimally distributing the currents $I_{c,j}$ among the tapes in the cable.

Fig. 6(c) shows the ratio of $I_{jk}/I_{c,j}$ in each tape during the current ramp. This ratio converges at operating current to nearly the same value such that all tapes operate with same current margin near critical operation. The current redistribution mostly occurs at the terminals and not along the length of the tape; only small amounts of current are shared across the face-to-face contact resistances. Because of this, it is important to maintain considerably small terminal resistances [31].

By accounting for the varying field (and thus varying I_c) across the tapes the critical current is 1.2 times larger than limiting the cable to the lowest single tape I_c. Furthermore, the cable critical current is 3.7 times larger in the conformal orientation (magnetic field parallel to tape faces) than it is in the 'worst orientation' (magnetic field perpendicular to tape faces).

Since all tapes are operating at approximately the same ratio of I/I_c~0.86 the total power dissipation in the cable can be estimated as shown in Eq. (4). The total dissipated power is modest and can be handled by modern cryogenic systems.

$$\frac{P}{L} = \frac{I^2R}{L} = \frac{IV_0}{L}\left(\frac{I}{I_c}\right)^n = .01\,\frac{\mathrm{W}}{\mathrm{m}} \tag{4}$$

D. Hall Effect, Inductive Coupling, Anisotropic Flux Pinning

The above circuit model is valid in the absence of Hall-like effects due to Lorentz forces and without inductive coupling between tapes. Those mechanisms play a strong role in current transfer. Future circuit models will take into account differential inductances between layers of tape to determine its effects during charging and discharging. We plan to experimentally measure the current distributions among tapes and the dynamics of redistribution during ramping in the experiments discussed in Sec. V.

Characterizing the dynamics of current sharing due to Hall effects requires a physical model of flux penetration within the ~1 μm-thick REBCO layer of the tape. Flux is pinned in high performance REBCO tapes by a number of pinning mechanisms [32]: anisotropic pinning from BZO nanorods along the *c*-axis, oxide-layer pinning in the *a-b* plane, and nanoparticle defects. There have been many efforts to develop (or measure) such a model, but there is no such understanding to date. Flux does penetrate – there is current-sharing in NI solenoids near the critical surface of the REBCO layer – but we do not know its dependence on the above dynamical variables.

V. Future Plans for Testing

The most fundamental experiment aims to test the behavior of current sharing within a straight length of NI tape-stack cable in a strong background field with its return leg in low-field. By aligning the *a-b* plane of the cable with a background field generated by an external magnet, current-redistribution due to the rise in dynamic resistivity, Hall-like effects, and inductive coupling can readily be investigated. Tests will be undertaken at the Helium-free test cryostat being fabricated at Accelerator Technology Corporation (ATC). This test cryostat is shown in Fig. 7 and is described in detail in a companion paper [33].

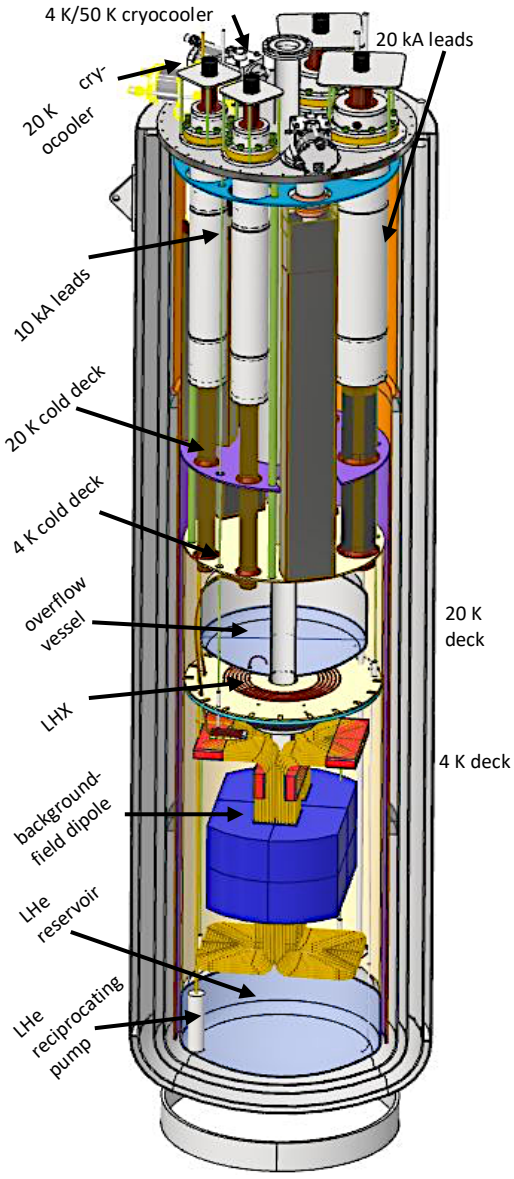

Fig. 6. ATC's Helium-free test cryostat [33]. The iron flux return for the 10 T background field magnet is shown in dark blue and its windings are shown in gold near the bottom of the cryostat.

The test cryostat contains a 10 T background-field dipole, with sufficient aperture to accommodate a single-turn bifilar winding of the tape-stack cable specified for the insert winding of the 18 T hybrid dipole of Fig. 2. We are developing a method by which to measure the currents in successive tapes in the U-turn of the specimen, so that current transfer can be quantified.

VI. Conclusion

A magnetic design has been presented for an 18 T hybrid dipole using a novel REBCO cable to fabricate the HTS insert winding. The novel REBCO cable is non-insulating and non-transposed; the geometry of the winding allows the cable to conform to the local magnetic field thus optimizing current carrying performance. Circuit models indicate that, under operation in such a field environment, currents will naturally redistribute to accommodate the non-uniform distribution of I_c across tapes in a cable. Stress, thermal, and field-harmonic analyses demonstrate the feasibility of such a magnet in many contexts. Future plans and experiments have been presented to validate this new technology and ultimately develop an 18 T hybrid dipole.

Acknowledgment

We thank Dr. Yifei Zhang for useful discussion and data on SuperPower Inc. REBCO tapes. We thank our lab staff, Tim Elliott and Ray Garrison, for their invaluable expertise and contributions to this work.

REFERENCES

[1] D. W. Hazelton, "SuperPower 2G HTS conductor", WAMHTS-1 workshop, Hamburg, May 2014.

[2] G. Majkic, R. Pratap, A. Xu, E. Galstyan and V. Selvamanickam, 'Over 15 MA/cm 2 of critical current density in 4.8 μm thick, Zr-doped (Gd,Y)Ba 2 Cu 3O x superconductor at 30 K, 3T', Sci. Reports, Vol. 8, 2018, Art. 6982.

[3] A. Ballarino, "Prospects for the use of HTS high field magnets for future accelerator facilities", *Proc. 5th Int'l. Particle Accel. Conf.*, Dresden, 2014, pp. 974-979.

[4] S. Hahn, K. Kim, K. Kim, X. Hu, T. Painter, I. Dixon, S. Kim, K.R. Bhattarai, S. Noguvhi, J. Jaroszynski and D.C. Larbalestier, "45.5-Tesla direct-current magnetic field generated with a high-temperature superconducting magnet". *Nature,* Vol. 570, 2019, pp. 496–499.

[5] S. Hahn, D. K. Park, J. Bascunan and Y. Iwasa, "HTS Pancake Coils Without Turn-to-Turn Insulation," *IEEE Trans. Appl. Supercond*., Vol. 21, No. 3, June 2011, pp. 1592-1595.

[6] X. Wang, T. Wang, E. Nakada, A. Ishiyama, R. Itoh, and S. Noguchi," Charging behavior in No-Insulation REBCO pancake coils," *IEEE Trans. Appl. Supercond*., Vol. 25, No. 3, June 2015, Art. no. 4601805.

[7] M. Takayasu, L. Chiesa, L. Bromberg and J. V. Minervini, "Electrical and mechanical characteristics of HTS twisted stacked-tape cable conductor", *IEEE Trans. Appl. Supercond*., Vol. 27, No 4, Jun. 2017, Art. no. 6900305.

[8] M. Takayasu, L. Chiesa, N. C. Allen, and J. V. Minervini, "Present status and recent developments of the twisted stacked-tape cable conductor," *IEEE Trans. Appl. Supercond*., Vol. 26, No. 2, Mar. 2016, Art. no. 6400210.

[9] W. Goldacker, F. Grilli, E. Pardo, A. Kario, S. I. Schlachter and M. Vojenčiak, "Roebel cables from REBCO coated conductors: a one-century-old concept for the superconductivity of the future", *Supercond. Sci. Technol*., Vol. 27, Aug. 2014, Art. no. 093001.

[10] L. Hao et al., "Conceptual Design and Optimisation of HTS Roebel Tapes," in IEEE Transactions on Applied Superconductivity, vol. 32, no. 4, pp. 1-5, June 2022

[11] D.C. van der Laan, J.D. Weiss, P. Noyes, U.P. Trociewitz, A. Godeke, D. Abraimov and D.C. Larbalestier, "Record current density of 344 A mm^2 at 4.2 K and 17 T in CORC accelerator magnet cables", *Supercond. Sci. Technol.,* Vol. 29, 2016, Art. no. 055009.

[12] Advanced Conductor Technologies LLC, "Superconducting cables and methods of making the same", U.S. *Patent* 10943712.

[13] Z. S Hartwig, R. F. Vieira, B. N Sorbom, R. A Badcock, M. Bajko, W. K. Beck, B. Castaldo, C. L Craighill, M. Davies, J. Estrada, V. Fry, T. Golfinopoulos, A. E Hubbard, J. H Irby, S. Kuznetsov, C. J. Lammi, P. C Michael, T. Mouratidis, R. A Murray, A. T Pfeiffer, S. Z Pierson, A. Radovinsky, M. D. Rowell, E. E Salazar, M. Segal, P. W Stahle, M. Takayasu, T. L. Toland and L. Zhou, "VIPER: an industrially scalable high-current high-temperature superconductor cable", *Supercond. Sci. Technol*., Vol. 33, No. 11, Oct. 2020, Art. no. 11LT01.

[14] J. S. Rogers, P. M. McIntyre, T. Elliott, G. D. May and C. T. Ratcliff, 'Strategies for conformal REBCO windings', *IOP Conference Series: Materials Science and Engineering*, 2022, Art. no. 012029.

[15] Y. Yan, C. Xin, M. Guan, H. Liu, Y. Tan, and T. Qu, "Screening current effect on the stress/strain distribution in REBCO high-field magnets: experimental verification & numerical analysis", *Supercond. Sci. Technol.* Vol. 33, No. 5, 2020, Art. no. 05LT02.

[16] K. R. Bhattarai, K. Kim, K. Kim, K. Radcliff, X. Hu, C. Im, T. Painter, I. Dixon, D. Larbalestier, S. G. Lee and S. Hahn "Understanding quench in no-insulation (NI) REBCO magnets through experiments and simulations", *Supercond. Sci. Technol*., Vol. 33, No. 3, Jan. 2020, Art. no. 035002.

[17] L. Cavallucci et al, "Quench in a pancake coil wound with REBCO Roebel cable: model and validation", *Supercond. Sci. Technol., 2021, 34 105002*

[18] T. Matsushita and M. Kiuchi, "Design of flux pinning property in REBCO coated conductors with artificial pinning centers", *Prog. in Supercond. and Cryo*., Vol. 20, No. 1, 2018, pp. 1-10.

[19] J. van Nugteren, G. Kirby, J. Murtomäki, G. DeRijk, L. Rossi and A. Stenvall, "Toward REBCO 20 T+ dipoles for accelerators," *IEEE Trans. Appl. Supercond*., Vol. 28, No. 4, June 2018, pp. 1-9.

[20] P. Ferracin, G. Ambrosio, D. Arbelaez , L. Brouwer , Member, IEEE, E. Barzi, L. Cooley, L. Garcia Fajardo, R. Gupta, M. Juchno, V. Kashikhin, V. Marinozzi, I. Novitski, E. Rochepault, J. Stern, A. Zlobin and N. Zucchi, "Towards 20 T hybrid accelerator dipole magnets," *IEEE Trans. Appl. Supercond*., Vol. 32, No. 6, pp. 1-6, Sept. 2022, Art no. 4000906.

[21] G. A. Kirby, J. van Nugteren, H. Bajas, V. Benda, A. Ballarino, M. Bajko, L. Bottura, K. Broekens, M. Canale, A. Chiuchiolo, L. Gentini, N. Peray, J. C. Perez, G. de Rijk, A. Rijllart, L. Rossi, J. Murtomaeki, J. Mazet, F-O. Pincot, G. Volpini, M. Durante, P. Fazilleau, C. Lorin, A. Stenvall, W. Goldacker, A. Kario and A. Usoskin, "First cold powering test of REBCO Roebel wound coil for the EuCARD2 Future Magnet Development Project", *IEEE Trans. Appl. Supercond.,* Vol. 27, No. 4, June 2017, Art. no. 4003307.

[22] X. Wang, D. Abraimov, D. Arbelaez, T. J. Bogdanof, L. Brouwer, S. Caspi, D. R Dietderich, J. DiMarco, A. Francis, L. Garcia-Fajardo, W. B. Ghiorso, S. A. Gourlay, H. C. Higley, M. Marchevsky, M. A. Maruszewski, C. S. Myers, S. O. Prestemon, T Shen, J. Taylor, R. Teyber, M. Turqueti, D. van der Laan and J. D. Weiss, "Development and performance of a 2.9 Tesla dipole magnet using high-temperature superconducting CORC(R) wires", *Supercond. Sci. Technol*., Vol. 34, No. 1, Art. no. 015012.

[23] P. M. McIntyre, J. Breitschopf, D. Chavez, T. Elliott, R. Garrison, J. Gerity, J. N. Kellams, and A. Sattarov "Cable-in-Conduit dipoles for the Ion Ring of JLEIC", *IEEE Trans. Appl. Superconduct*. Vol. 29, No. 5, Aug. 2019, Art. no. 4004806.

[24] R. Gupta, R. Scanlan, A. K. Ghosh, R. J. Weggel, R. Palmer, M. D. Anerella and J. Schmalzle, "Low temperature superconductor and aligned high temperature superconductor magnetic dipole system and method for producing high magnetic fields", U.S. *Patent* 9793036

[25] D. Uglietti, R. Kangab, R. Weschea and F. Grillic, "Non-twisted stacks of coated conductors for magnets: Analysis of inductance and AC losses", *Cryogenics*, Vol. 110, Sept. 2020, Art. no. 103118.

[26] https://www.superpower-inc.com/

[27] G. D. May, J. S. Rogers, and P. M. McIntyre, "Nb_3Sn CIC for outsert windings of hybrid dipoles", *IEEE Trans. Appl. Supercond*., 2022, *to be published*

[28] A. C. A. Martınez., Q. Ji, S. O. Prestemon, X. Wang and G. H. I. Maury Cuna, 'An electric-circuit model on the inter-tape contact resistance and current sharing for REBCO cable and magnet applications', *IEEE Trans. Appl. Supercond*., Vol. 27, No. 4, June 2017, Art no. 6900305.

[29] J. Lu, K. Han, W. R. Sheppard, Y. L. Viouchkov, K. W. Pickard and W. D. Markiewicz, "Lap joint resistance of YBCO coated conductors", *IEEE Trans. Appl. Supercond.*, Vol. 21, No. 3, June 2011, pp. 3009-3012,

[30] J. Lu, R. Goddard, K. Han and S. Hahn, "Contact resistance between two REBCO tapes under load and load-cycles", *Physics: Instrumentation and Detectors*, Jan. 2017, arXiv:1701.00447.

[31] G.P. Willering, D.C. van der Laan, H.W. Weijers, P.D. Noyes, G.E. Mille1, and Y. Viouchkov, "Effect of variations in terminal contact resistances on the current distribution in high-temperature superconducting cables", Supercond. Sci. Technol. 28 035001, Jan. 2015

[32] A. Xu, V. Braccini, J. Jaroszynski, Y. Xin, and D. C. Larbalestier, "Role of weak uncorrelated pinning introduced by $BaZrO_3$ nanorods at low-temperature in (Y,Gd)Ba_2Cu_3Ox thin films", *Phys. Rev*., Vol. B 86, Sept. 2012, Art. no.115416.[

[33] C.D. Coats, J.S. Rogers Jr., and P.M. McIntyre, "Design of a Helium-Free Test Cryostat for Superconducting Wires, Cables, and Windings", *IEEE Trans. Appl. Supercond*., 2022, *to be published*